EVALUATION OF ASSERT-PV V3R1 VOID FRACTION PREDICTIONS AGAINST THE OECD/NEA BFBT BENCHMARK DATA

K. H. Leung and D. R. Novog
McMaster University, Hamilton, Ontario, Canada
leungk4@mcmaster.ca

Abstract

The subchannel code ASSERT, developed by Atomic Energy of Canada Limited, is assessed against the steady-state void fraction cases from the OECD/NEA BFBT benchmark. Preliminary void fraction predictions from 84 BWR bundle tests were compared to experimentally reported values, and 45.2% of the simulated data fell within the reported experimental error. Overall, the code was able to predict the void fraction to within ±0.10 of the experimental value about 95% of the time, although calculations of the corner subchannels were not as accurate, falling within ±0.10 of the experimental value only 69.3% of the time. An analysis of four isolated cases suggested that the code over predicts the void fraction in the corner and side channels for cases at low pressure (~1.0 MPa). A sensitivity analysis on one case demonstrated that the boundary condition uncertainties could affect the void fraction by up to 0.026. Accounting for the boundary condition uncertainties in this case increased the number of subchannel predictions falling within experimental error from 34 to 46. Additionally it was determined that for the case examined the boundary condition uncertainty most significantly affected the central subchannel void fraction prediction.

1. Introduction

The cores of nuclear reactors consist of a number of parallel fuel rods that convect heat to a liquid coolant passing over them. The spaces in between these rods as illustrated in Figure 1 are known as subchannels, and the prediction of void fraction in the fuel channels is an important aspect of thermalhydraulic safety analyses. The void fraction, α, of a channel or subchannel is defined as the fraction of the volume which is occupied by water vapour as opposed to liquid. The void reactivity coefficient and Critical Heat Flux (CHF) are two of the phenomena which depend on the void fraction of the coolant, and since the understanding of both plays a major role in nuclear safety, it is essential for the void fraction to be accurately modeled. In practice, the void fraction is averaged either over the entire fuel bundle volume or in an individual subchannel over a period of time.

Current codes are capable of predicting the bundle averaged void fraction fairly well, however subchannel level predictions still have room for improvement since the theoretical basis of void formation, distribution and subchannel mixing are not yet fully understood. Factors such as subchannel cross-flows and a lack of high resolution full-scale data under nuclear reactor operating conditions have been cited as reasons why a comprehensive model has not yet been developed [1]. One of the current studies underway is the Organization of Economic Cooperation and Development / Nuclear Energy Agency (OECD/NEA) Boiling Water Reactor Full-Size-Fine-Mesh Bundle Test (BFBT) benchmark. The aim of this benchmark is to compare

accuracy of the available models which are currently used in subchannel codes, and to evaluate the different uncertainty methodologies in use. The BFBT data were collected by the NUclear Power Energy Corporation (NUPEC) of Japan, and consists of high resolution X-Ray densitometer measurements of full scale electrically heated BWR type bundles [1].

The Advanced Solution of Subchannel Equations in Reactor Thermalhydraulics (ASSERT) code was developed by AECL and is primarily used to predict the thermalhydraulic behaviour of CANDU fuel channels. However, its extensive and general theoretical approach makes it well suited to study BWR type geometries. ASSERT is a 1-D code which models the mass, momentum and energy equations in each subchannel of a fuel bundle. A drift-flux model based on the difference between the vapour and liquid velocities is used, while empirical correlations model friction factors, heat transfer coefficients and subchannel interactions [2]. The code has been used in the past not only to model CANDU fuel channels under normal operating conditions, but also in scenarios where the pressure tubes are crept [2] or when evaluating the void distributions [3] or the CHF characteristics [4] of different bundle designs.

This paper documents the preliminary findings in the application of ASSERT-PV V3R1 for predicting the void distribution in vertical BWR style bundles. Specifically, the code will be used to simulate the steady-state void fraction tests conducted as part of the BFBT exercises.

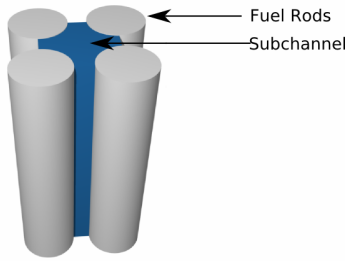

Figure 1 - Subchannel Definition

2. Methodology

2.1. Facility and Test Description

The NUPEC data were acquired in the early 1990s in a full sized facility using electric rod simulators. The characteristics of the test facility are listed in Table 1, and tests were run at conditions which mimic what would typically be found in BWR during both normal operating conditions and transient accident scenarios [1].

Table 1 – NUPEC Test Facility Details (left) and Experimental Conditions (right) [1].

Parameter	Quantity
Maximum Power (MW)	12
Maximum Mass Flux (kg / m^2-s)	2130
Maximum Pressure (MPa)	10.3
Number of Fuel Rods	62
Rod Pitch (mm)	16.2
Fuel Rod Diameter (mm)	12.3
Number of Water Rods	2
Water Rod Diameter (mm)	15
Heated Length (mm)	3708

Quantity	Test Range
Power (MW)	0.23 – 6.48
Mass Flow (kg/s)	2.78 – 19.34
Pressure (MPa)	0.95 – 8.65
Inlet Subcooling (kJ/kg)	44.3 - 128.4
Outlet Mass Quality (%)	2 - 25

The simulations being analyzed in this paper are conducted on the bundle type illustrated in Figure 2 (left). The bundle sat in a test loop filled with demineralised light water, and was supported by spacer grids. Each spacer grid was determined by the international benchmark team to have an axial form loss coefficient of k = 1.2. The bundle has a non-uniform power profile in both the radial and axial directions. The relative power profile is illustrated in Figure 2 (left), while the axial power profile is illustrated in Figure 3. Five types of subchannels are also identified in Figure 2. The total flow area for this bundle configuration is 9781 mm^2 and the two shaded fuel rods in the center are water rods and are not heated.

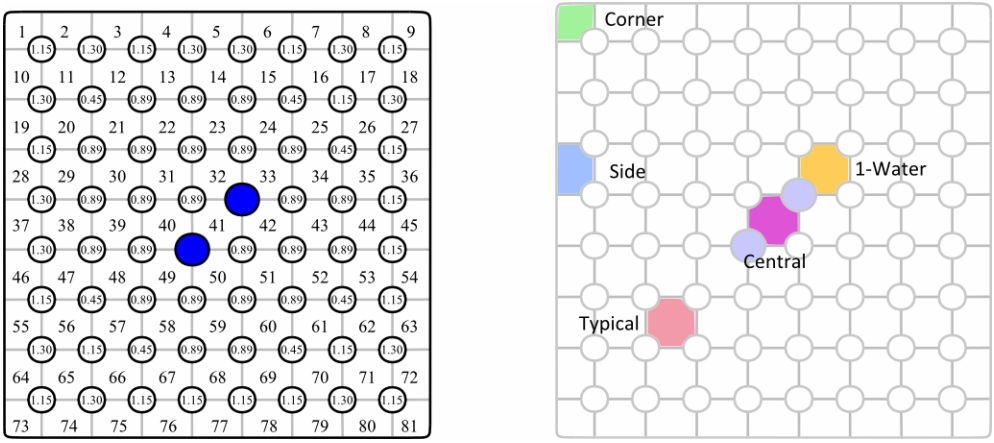

Figure 2 - Bundle cross section with relative rod power and subchannel indices listed (left) and subchannel types of interest (right).

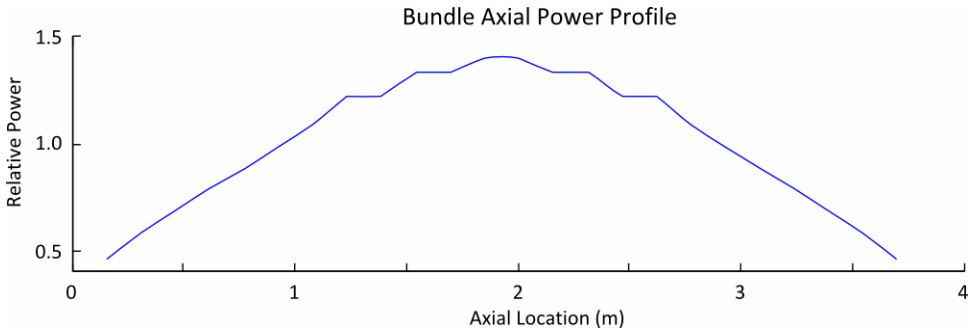

Figure 3 - Axial power profile of the test bundle.

X-Ray densitometers measure the chordal void fraction at various points along the length of the bundle, while an X-Ray CT scanner takes high resolution measurements at the top of the bundle just before the outlet. In this study the results obtained by ASSERT will be compared to the outlet void fraction measured by the X-Ray CT scanner. A total of 86 steady-state cases were attempted with different combinations of bundle power, mass flow rate, pressure and inlet subcooling. Four cases have been singled out for a more extensive study. These cases were selected to illustrate the difficulties which the code has during low flow rate – low power conditions.

2.2. ASSERT Model

Each of the 81 subchannels and 62 fuel rods are modeled in ASSERT using 20 axial nodes, and the simulations are performed at steady-state conditions. The flow area, hydraulic diameter, and the wetted and heated perimeters for each subchannel are computed and modelled in the axial direction. Junction widths, angles and subchannel centroid distances are determined in the planar direction. A symmetry condition is deliberately avoided since the experimental results do not exhibit symmetrical characteristics. The outlet pressure, mass flux, heat flux and inlet temperature are all derived from the experiment and used as boundary conditions in ASSERT. The empirical correlations used and their justification are listed in Table 3.

Table 2 - Model Correlation Selection

Parameter	Correlation	Justification
Single Phase Friction Factor	Colebrook-White	Valid for flows in the turbulent regime. The Reynolds Number in subchannels is > 40,000.
Two-Phase Friction Multiplier	Friedel	Collier & Thome recommend the use of this correlation for two phase flows where $\mu_f / \mu_g < 1000$ [5].
Single Phase Heat Transfer Model	Dittus-Boelter	Valid for turbulent flows and Prandtl numbers between 0.7 and 120. The Prandtl number for this case is between 0.8 and 1.8.
Two-Phase Heat Transfer Model	Ahmad	Valid for steam-water mixtures under BWR and PWR pressures and mass fluxes [2].
Mixing & Void Distribution	Carlucci	Developed based on data for vertical steam-water flows under BWR & PWR conditions [6].
Equilibrium Void Fraction	Rowe	Developed based on BWR & PWR geometries and mass fluxes [2].

2.3. Wilks' Formula

Every measurement typically has an uncertainty associated with it. One of the problems with attempting to simulate experiments is that the actual experimental conditions which form the boundary conditions for the simulations are never truly known, and the variable of interest, void fraction, is also subjected to significant measurement errors. In the context of this study, the uncertainty of the void fraction measurements is given by the benchmark organizers to be ±0.03 of the measured value, and applying this uncertainty to the analysis is straight forward. However, there are additional uncertainties associated with each of the pressure, flow, power and temperature measurements taken, and these are listed in Table 3.

Table 3 - Experimental Uncertainty

Quantity	Accuracy	Distribution
Pressure	1.00%	Normal
Mass Flow Rate	1.00%	Normal
Power	1.50%	Normal
Inlet Temperature	1.50 C	Flat
Subchannel Void Fraction	0.03	Normal

In order to properly account for these uncertainties, an analysis must be conducted to determine the sensitivity of the void fraction to the variation of the boundary conditions. Unfortunately, owing to the complex and non-linear nature of the constituent equations required to describe the system, propagating the boundary condition uncertainties through the code is not necessarily a trivial task. The overall error structure in the void fraction predictions contains the following components:

- Error in the code predictions resulting from imperfect theoretical formulations and simplifications as well as model parameter uncertainties.
- Error in the void fraction measurement itself
- Error in the inlet boundary conditions

The focus of this study will be to assess the code uncertainty while considering the errors in measurements of void as well as in the boundary conditions. The simplest method of determining the effect of the boundary conditions on the output would be to use the Monte Carlo method, which may require that the code be run hundreds to thousands of times, randomly selecting boundary conditions for each simulation in order to generate a output distribution. Ordered statistics – specifically Wilks' formula – may be used to significantly reduce the computational effort required. Although the theory and derivation of this formula is beyond the scope of this study, Wilks' formula essentially yields a minimum number of code runs required based on the distribution shape, probability and confidence level desired [7]. For the purposes of this study, in order to determine the 95^{th} percentile bounds of the simulated void fraction to confidence of 95%, 93 code runs are required assuming a two-tailed distribution. Based upon these results an estimate was made for the relative contribution of input boundary conditions on the void fraction estimates obtained from ASSERT.

3. Results

3.1. Overall Code Accuracy

Overall, the ASSERT results are in excellent agreement with the experiments. There were two cases that were attempted but failed, and they were characterized by low pressure (0.98 MPa), low flow (2.80 kg/s) and low power (0.23 – 0.32 MW) boundary conditions. The void fraction in each of the subchannels of the successfully run cases are compared against the experimental data, and as Figure 4 illustrates, approximately 95% of the simulated data fell within the bounds $-0.10 \le \delta \le 0.10$, where δ is simply the difference between the simulated and experimental void fraction defined in equation (1).

$$\delta = \alpha_{SIM} - \alpha_{EXP} \tag{1}$$

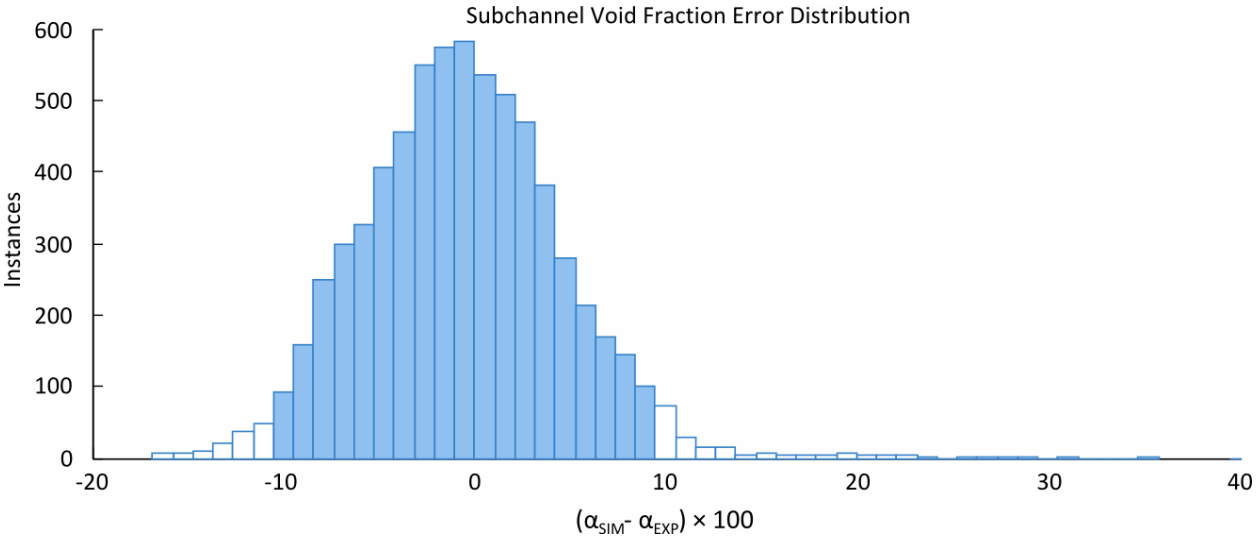

Figure 4 – Subchannel Void Fraction Error Histogram. The shaded region contains 95% of the data points.

Table 4 - ASSERT Subchannel Void Fraction Prediction Accuracy

Subchannel Type	Number of points where $\delta \le 0.03$		Number of points where $\delta \le 0.05$		Number of points where $\delta \le 0.10$		$\overline{\delta} \times 100$	$\sigma_\delta \times 100$	N_{Points}
Typical	1676	(47.5%)	2481	(70.3%)	3472	(98.4%)	-1.6337	4.2749	3528
Side	970	(41.2%)	1490	(63.4%)	2204	(93.7%)	0.6052	5.5472	2352
1-Water	286	(56.7%)	401	(79.6%)	501	(99.4%)	-0.2909	3.8668	504
Corner	101	(30.1%)	156	(46.4%)	233	(69.3%)	0.7924	9.7107	336
Central	43	(51.2%)	56	(66.7%)	81	(96.4%)	-1.4446	4.5193	84
All Subchannel Types	3076	(45.2%)	4584	(67.4%)	6491	(95.4%)	-0.6382	5.2245	6804

Sorting the data by subchannel type as in Table 4 demonstrates that the code accuracy is dependent on the location of the subchannel within the bundle. Note that in the table, $\overline{\delta}$ and σ_δ represent the average and standard deviation of the subchannel data being compared. Positive values of $\overline{\delta}$ in the side and corner subchannel types suggest that the code may have a tendency to overpredict the void fraction in these regions. Although the $\overline{\delta}$ values are less than the measurement error, the large σ_δ values imply that a substantial number of the points fall outside of experimental uncertainty. Only 69.3% of the corner channels simulated fell within $\delta \le 0.10$, which together with the high standard deviation suggest that the code has difficulty predicting the void fraction in the corners.

The void profiles in Figure 5 illustrate the qualitative characteristics of a case with low-pressure, flow and bundle power. From the figure, several details are evident:

- The void fraction in the corner and side subchannels is over-predicted in this case – however this characteristic is specific to this case as in cases at higher pressure, power and flow, the void in these subchannels is under-predicted.

- While the void in the "typical" subchannels seems overpredicted, the void in the cooler "central" subchannel is underpredicted. This insinuates that the void fraction problems in the corner are not only a function of power, but some other parameter. This may also suggest a problem in the two-phase mixing coefficients at these low flow-low power conditions.

- The relatively flat simulated void profile – despite the variation in subchannel power - suggests that the mixing coefficients are poorly predicted under low flow conditions.

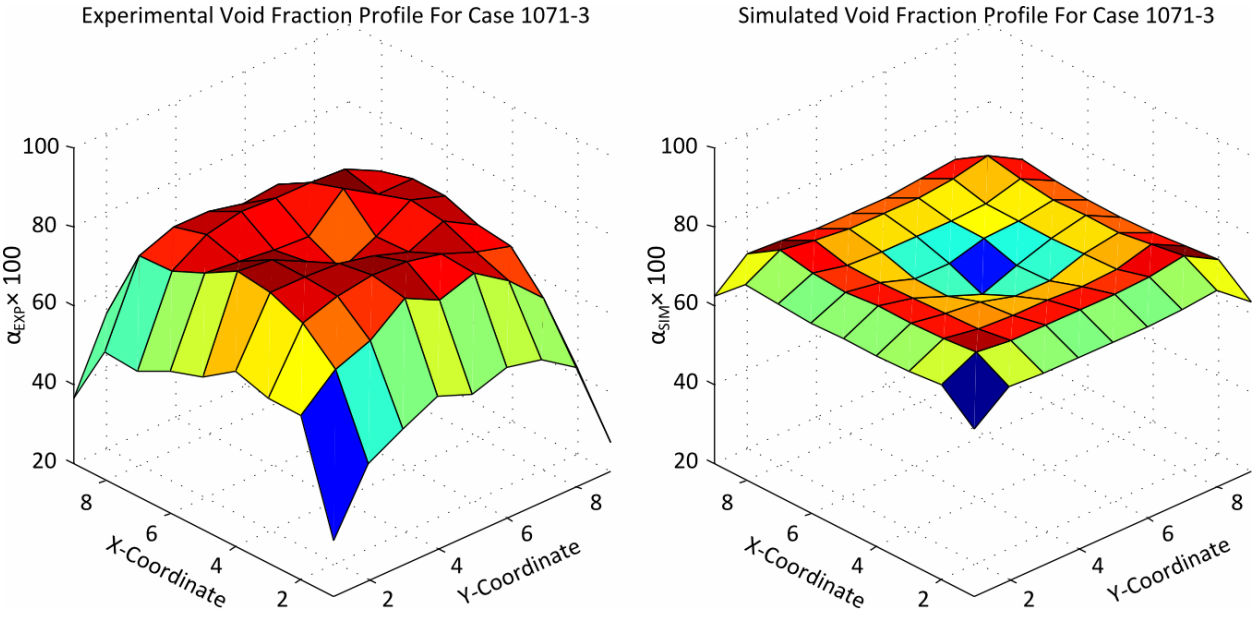

Figure 5 - Experimental (left) and Simulated (right) Void Fraction Profile for Case 1071-3.

3.2. Accuracy of Selected Cases

Four cases were selected for further analysis to highlight the effects of the boundary conditions. The conditions for these cases are listed in Table 5. Cases 1071-3 (low flow, low power, low pressure), 1071-13 (high flow, high power, low pressure), while 1071-69 (low flow, low power, high pressure) and 1071-86 (high flow, high power, high pressure).

Table 5 - Selected cases for detailed analysis.

	Test Number			
	1071-3	**1071-13**	**1071-69**	**1071-86**
Inlet Pressure [MPa]	0.967	1.234	8.609	8.681
Mass Flow Rate [kg/s]	2.817	15.23	2.778	15.17
Bundle Power [MW]	0.430	6.320	0.220	4.630
Inlet Subcooling [kJ/kg]	46.30	88.50	51.30	53.30

Figure 6 and Figure 7 illustrate the predicted versus measured void fractions of each subchannel in the selected test cases. The two plots suggest that the over prediction in the corner and side subchannels is most significant under low pressure conditions, and is reduced when pressure is increased. In the two high pressure cases tested, 153 of the 162 or 94% of points fell within ±0.10 of the experimental value, which is consistent with the data presented in the previous section. However, in the low pressure cases, each of the corner subchannels were significantly over predicted, while only 111 of 162 points or 68.5% of points fell with ±0.10 of the experimental value.

This inaccurate result for the low pressure cases are likely caused by the choice of mixing and void distribution correlation. Although the Carlucci correlation was developed specifically for steam-water flows under BWR and PWR operating conditions, the experimental data which it is based off of only spans between 5.0 and 16.0 MPa whereas the boundary conditions in the low pressure cases were 0.97 and 1.23 MPa. The problem is further compounded in case 1071-3, as the mass flux range of the correlation data is between 680 – 6000 kg/m^{2}s while the test was run at 285 kg/m^{2}s.

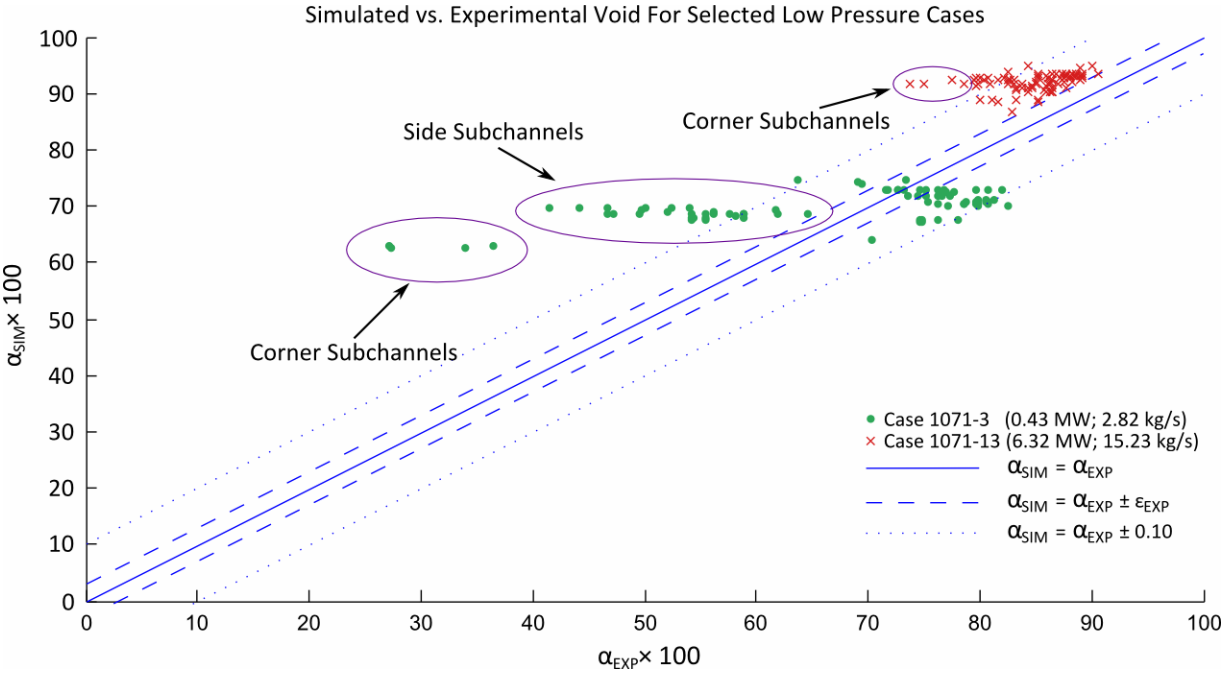

Figure 6 - Predicted vs. Measured Void Fraction Graphs for Selected Low Pressure Cases

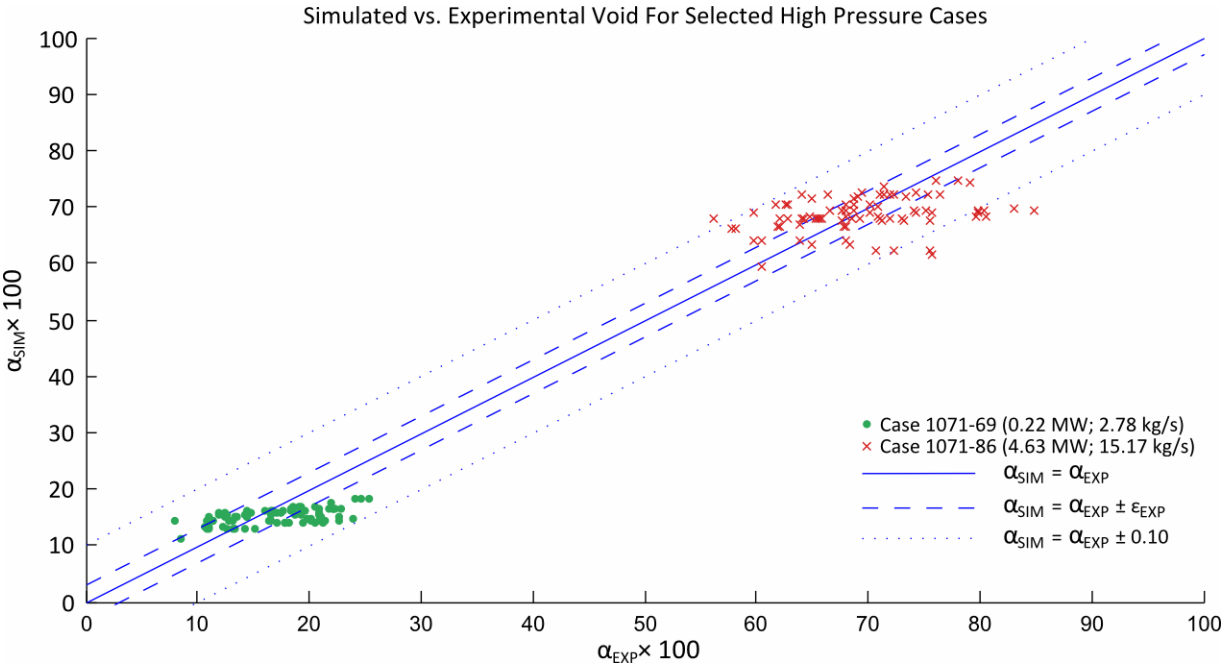

Figure 7 - Predicted vs. Measured Void Fraction Graphs for Selected High Pressure Cases

3.3. Sensitivity to Boundary Condition Uncertainty

The sensitivity of the code predictions to the boundary condition uncertainty may be assessed using Wilks' formula. In the study, one specific case was taken – case 1071-86 – and 93 sets of boundary conditions are randomly generated for the inlet temperature, outlet pressure, mass flow rate and bundle power based on the distributions indicated in Table 3. The variation of these conditions is illustrated in Figure 8.

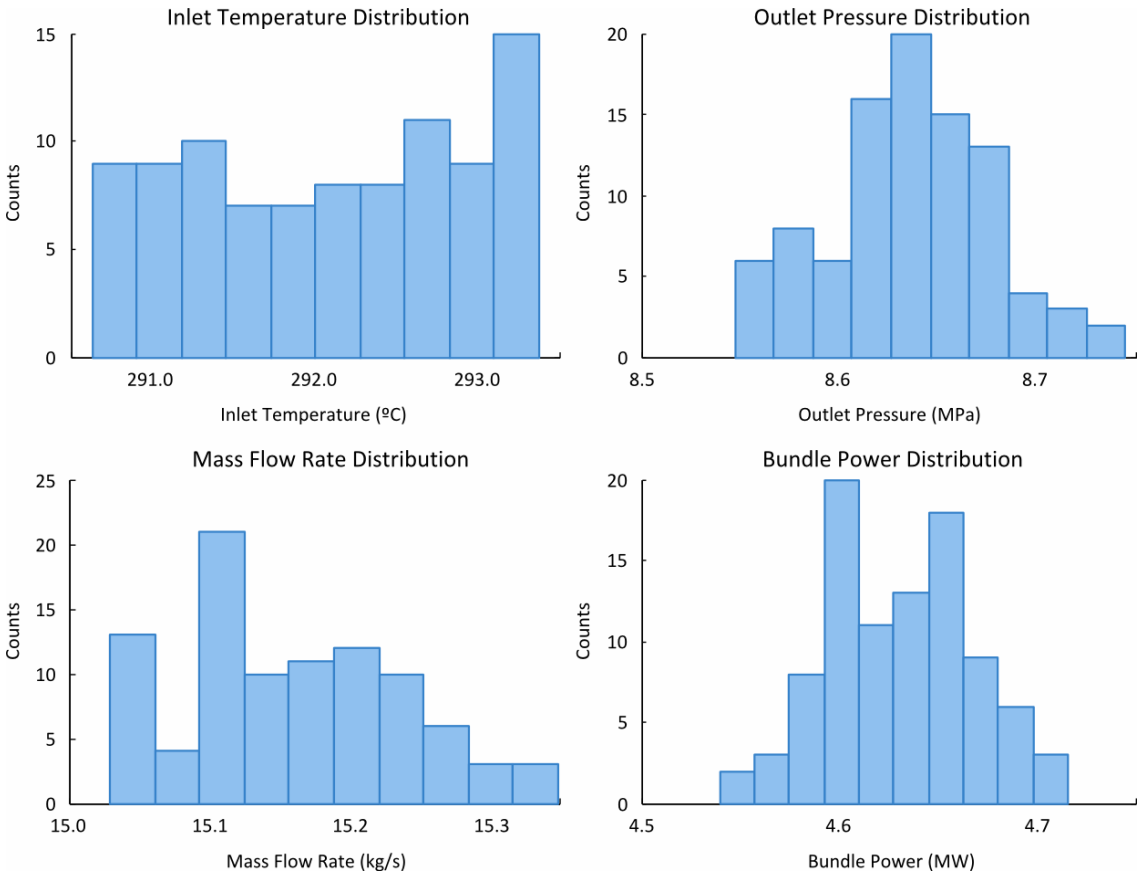

Figure 8 – Distribution of Boundary Conditions

A subchannel-by-subchannel comparison of the experimental and ASSERT results for this case are provided in Figure 9. In the figure, the reported experimental values are denoted by the blue dots, surrounded by uncertainty bars representing the measurement error. The thicker rectangles represent the possible range of simulated values derived by running the code for each of the sets of boundary conditions generated. The results for each subchannel are placed in numerical order such that $\alpha_1 < \alpha_2 < \ldots \alpha_N$. α_2 and α_{N-1} are then plotted as the lower and upper bounds for the predicted void fraction of that particular subchannel. These bounds represent the two-tailed 95% / 95% bounds found using Wilks' formula.

The influence of the boundary condition uncertainty on the code predictions is evident when the number of simulated points falling within the experimental error is considered. From the data presented in Figure 7, when the code was run using strictly the boundary conditions provided,

only 34 of the 81 subchannels void fraction predictions were between the lower and upper experimental bounds. Consideration of the uncertainty of the boundary conditions gives a range of possible void fraction predictions, the experimental uncertainty and the prediction uncertainty was found to overlap in 46 of the subchannels.

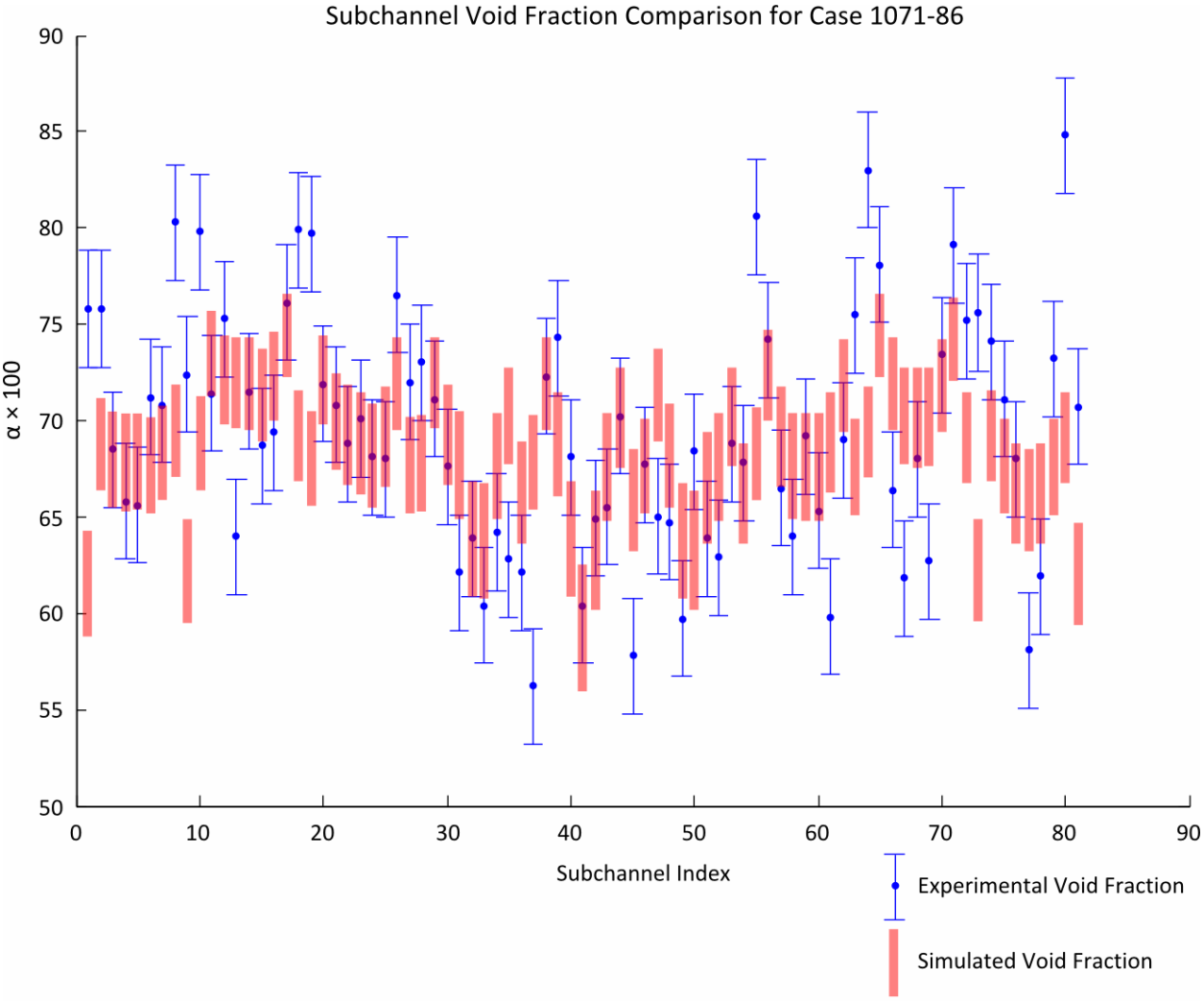

Figure 9 - Subchannel Void Fraction Comparison for Case 1071-86 with Experimental and Simulated Uncertainty Bounds

Figure 10 plots the size of each of the red bands as a function of their radial position within the bundle. The subchannels near the center of the bundle are the most sensitive to the boundary condition variations, while subchannels adjacent to the side subchannels are least sensitive. On average, the size of each of the uncertainty bands derived is 0.0263, which represents a level of uncertainty caused by the boundary conditions about half that of the experimental error.

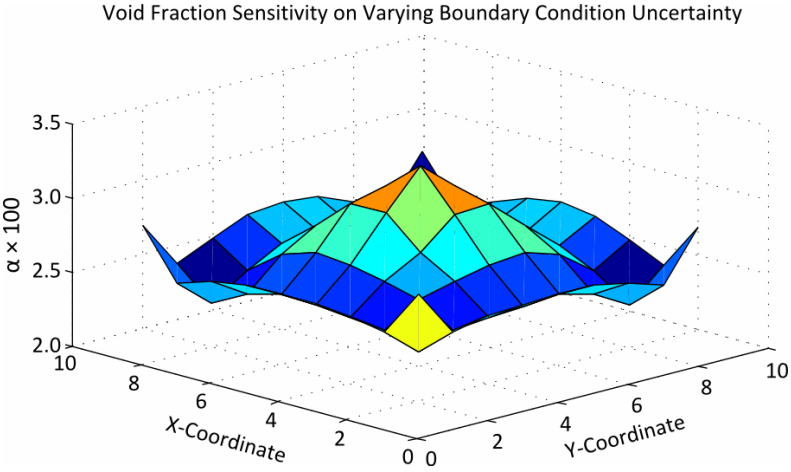

Figure 10 - Sensitivity Band Size Dependence of Radial Position Within the Bundle.

4. Conclusions

We have applied the ASSERT subchannel code to predicting the steady-state void fraction of BWR bundles on a subchannel basis. A preliminary analysis of 84 cases determined that approximately 95% of the points fell within ±0.10 of the measured value. Cases run at low pressure, power and mass fluxes either failed or yielded poor predictions. In one particular case run, the void fraction was over-predicted in one of the corner subchannels by over 0.35, and we conclude this implies that in such cases there exists a phenomena requiring further study. This is expected since the void mixing relationships inherent in ASSERT were derived from higher pressure data. Hence further work to develop low pressure mixing models, or alternatively a more universally applicable correlation may be needed.

We have also demonstrated in this study that boundary condition uncertainty contributes about 0.0263 to the code void fraction uncertainty for one particular case. The boundary condition uncertainties have the greatest effects on the corner and central subchannels, which is where a majority of the void fraction inaccuracy takes place.

5. References

[1] B. Neykov, F. Aydogan, L. Hochreiter, K. Ivanov, H. Utsuno, K. Fumio, *NUPEC BWR Full-Size Fine-Mesh Bundle Test (BFBT) Benchmark. Volume 1: Specifications*, NEA/NSC/DOC(2005)5.

[2] ASSERT-PV V3R1 Theory Manual. Atomic Energy of Canada Limited, Mississauga, Canada, 2007.

[3] Park, J. W., A subchannel analysis of DUPIC fuel bundle for the CANDU reactor, *Annals of Nuclear Energy*, 26, pp. 29-46, 1999.

[4] Leung, L. K. H., Effect of CANDU Bundle Geometry Variation on Dryout Power, *Journal of Engineering for Gas Turbines and Power*, 131, 10 pages, 2009.

[5] Collier, J. G., and Thome, J. R., Convective Boiling and Condensation, Oxford Science Publications, New York, United States of America, 2001.

[6] Carlucci, L. N., Hammouda, N., and Rowe, D. S., Two-phase turbulent mixing and buoyancy drift in rod bundles, *Nuc. Eng. Des.,* 227, pp. 65-84, 2004.

[7] Glaeser, H., GRS method for uncertainty and sensitivity evaluation of code results and applications, *Science and Technology of Nuclear Installations*, vol. 2008, 7 pages, 2008.